The Blunt-Leading-Edge Problem in Hypersonic Flow

HAKURO OGUCHI*
University of Tokyo, Komaba, Meguro-ku, Tokyo

The present paper is mainly concerned with the hypersonic flow over a flat plate with a blunt nose. The analysis is based on the flow model in which the flow field behind the shock wave may be divided into two regions: the inviscid-hypersonic-flow region and the entropy layer, across which the pressure has no appreciable change. The equations for the entropy layer can be reduced to those of the usual boundary-layer problem with the exception that the outer edge of the entropy layer, as well as the pressure remain unknown. These unknowns are determined so as to approximately match the entropy-layer solution with the inviscid hypersonic solution in which the shock wave has the shape of the 2/3-power law of the distance from the leading edge. The assumed flow model is shown to be valid over a restricted range depending on the wall-to-stagnation temperature ratio and $Re_t/M\sqrt{C}$ (where Re_t is the Reynolds number based on half the thickness of nose t, M the freestream Mach number, and C the Chapman-Rubesin constant. Actual calculations have been carried out for the case with typical values of $Re_t/M\sqrt{C}$ and the wall-to-stagnation temperature ratio T_w/T_0. The calculated values for both the surface pressure and heat-transfer rate are compared with the experimental data. As regards surface pressure in particular, a satisfactory agreement with the data is obtained. The validity of the assumptions upon which the present analysis is based has been examined from the numerical results, and the region of the validity has been found to extend over a certain large range of the nondimensional distance from the leading edge.

Nomenclature

a = nondimensional shock-layer-thickness parameter
a^* = the reference value of a when the parameter $Re_t/M\sqrt{C}$ is very large
A = constant
C_f = skin-friction coefficient $(\mu\partial u/\partial y)_w/(\rho_\infty u_\infty{}^2/2)$
C_H = surface heat-transfer coefficient $(\lambda\partial T/\partial y)_w/\rho_\infty u_\infty(H_\infty - H_w) = q/\rho_\infty u_\infty(H_\infty - H_w)$
C_p = specific heat of the gas at constant pressure
C = Chapman-Rubesin constant
f = function whose derivative $\partial f/\partial\eta$ is u/u_E ($\approx u/u_\infty$)
F = function of θ ($= y/y_S$)
h = specific enthalpy
H = total specific enthalpy
I = integral $\int_0^\infty\{(T_w/T_0) + [1 - (T_w/T_0)]\Theta - f_\eta{}^2\}\,d\eta$
k = nose-drag coefficient defined by $D_N/\frac{1}{2}\rho_\infty u_\infty{}^2\cdot 2t$ where D_N is the nose drag
K = value of p/p_S as $\theta \to 0$
M = freestream Mach number
p = pressure
Pr = Prandtl number
q = local surface heat-transfer rate
Re_x = Reynolds number $= \rho_\infty u_\infty x/M_\infty$
Re_t = Reynolds number $= \rho_\infty u_\infty t/M_\infty$
t = half the thickness of the nose
T = temperature
u,v = velocity components parallel to the x and y axes
x,y = rectangular coordinates in directions parallel and normal, respectively, to the freestream direction, with the origin at the nose shoulder
y_E = y-coordinate of the outer edge of entropy layer
y_S = y-coordinate of shock wave
β = constant appearing in the asymptotic form of f as η is very large ($f \approx \eta - \beta$)
γ = specific-heat ratio
δ = constant $= (4/9)^{1/2}\sqrt{\gamma/(\gamma+1)}K^{(2-\gamma/2\gamma)}$
ϵ = $(\gamma - 1)/(\gamma + 1)$
Ψ = stream function
θ = y/y_S
Θ = $(H - H_w)/(H_E - H_w) \approx (H - H_w)/(H_\infty - H_w)$
μ = viscosity coefficient of the gas
λ = thermal conductivity of the gas
ξ,η = spatial variables defined by Eqs. (2.6a) and (2.6b), respectively
ρ = density
$\bar{\chi}$ = hypersonic interaction parameter $= M^3\sqrt{C/Re_x}$

Subscripts

E = pertaining to the outer edge of entropy layer
S = immediately behind the shock wave
0 = freestream stagnation condition for the temperature
w = pertaining to the wall condition
∞ = pertaining to the freestream condition

Received by IAS June 5, 1962; revision received November 29, 1962. The work was carried out at the Graduate School of Aeronautical Engineering, Cornell University, while the author was on leave of absence from University of Tokyo. The author would like to express his sincere thanks to Prof. W. R. Sears and his colleagues of the school for their helpful suggestions and kind advice. The author would also like to express appreciation to Prof. R. F. Probstein of Brown University and Dr. H. K. Cheng of the Cornell Aeronautical Lab., Inc. for their helpful suggestions and stimulating discussions during this investigation.

* Professor, Aeronautical Research Institute, University of Tokyo.

I. Introduction

As is well known, the effects of the blunt leading edge as well as the boundary layer are important in hypersonic-flow problems of slender bodies. In order to investigate the essential characteristics of these effects on the flow properties, we consider as a simple example a flat plate with a blunt nose, placed in a freestream with no incidence.

In earlier stages of the investigation of the problem, inviscid flow analyses incorporated with blast-wave theory brought many fruitful results.[1–5] However, such analyses fail to clarify the details of the flow behavior in the region close to the surface, because the hypersonic-small-disturbance approximation on which the inviscid analysis is based is no longer applicable in the neighborhood of the surface.[6,7] Indeed, the transverse-momentum equation, with which the hypersonic approximation is mainly concerned, degenerates into the trivial equation $\partial p/\partial y \approx 0$ (where p is the pressure

and y the distance measured from the surface) in a region close to the surface.

According to the inviscid analysis for hypersonic flow over a plane flat plate with a blunt nose (for example, see Ref. 2), the shock wave has a shape which is given by $y_S \sim x^{2/3}$ (where x is the distance from the leading edge). The solution which is identical with the constant-energy-blast-wave solution gives the vanishing density and infinitely high temperature on the surface. Such anomalous behaviors that the inviscid solution suggests are associated with the appearance of a high-entropy layer near the surface. Most of the fluid particles within the entropy layer may be considered to have initially passed through a strong portion of the shock wave near the leading edge. Actually both the temperature and density should be finite on the surface as discussed in Ref. 8, so that such an apparent singularity of flow variables on the surface should diminish in taking into account the viscosity effect. In the absence of the viscosity the entropy layer may be assumed to be generated mostly due to the drag imparted by the blunt nose. Therefore the surface pressure and/or shock-wave shape are well estimated from the blast-wave analogy by an appropriate choice of the nose-drag coefficient without any detailed knowledge of the flow within the entropy layer.[3] However, the determination of the nose-drag coefficient which represents the nose-bluntness effect is rather empirical. In order to estimate the effects of both the nose bluntness and viscosity it should be required to make clearer the flow behavior within the high-entropy layer. Therefore, for the entropy layer the longitudinal-, as well as transverse-momentum equations must be dealt with, including the viscosity effect which in general plays a significant role in the region very close to the surface.

The combined effects of both the nose bluntness and boundary layer on the characteristic aerodynamic quantities were investigated by several authors,[9-12] mainly on the basis of experimental works. Recently a group at the Cornell Aeronautical Lab. presented an analysis to clarify considerably the combined effects of both nose bluntness and boundary-layer displacement, together with concurrent experimental works.[13, 14] The analysis was carried out on the basis of a flow model in which the flow field behind the shock wave is composed of three regions: the infinitely thin hypersonic region, the boundary layer, and an in-between inviscid entropy layer. Such a theoretical approach could remedy the break down of the inviscid hypersonic approximation within the entropy layer, because the longitudinal-, as well as transverse-momentum equations were taken into account. The results concerning the heat transfer well explain the experimental data. However, the analysis still involves some uncertainty in the determination of the nose-drag coefficient, as does any analysis incorporating the blast-wave analogy.

In the present paper we consider only the region which is not so far downstream from the leading edge that the boundary layer is confined within the entropy layer. We shall examine a possibility to match consistently the solution for the inviscid hypersonic region to the solution for the entropy layer. It will be shown that such a matching can be done approximately over a certain range whose extent depends on both parameters $M\sqrt{C}/\sqrt{Re_t}$ (where M is the freestream Mach number, Re_t the Reynolds number based on half a thickness of the nose t, and C is the Chapman-Rubesin constant) and T_w/T_0, the wall-to-stagnation temperature ratio.

II. The Solution for the Entropy Layer and the Condition on the Outer Edge of the Entropy Layer

As will be justified in the following analysis, the shock wave which is generated due to the nose bluntness is found to be approximately in the form of $y_S \sim x^{2/3}$. For such a shock wave the inviscid analysis[15, 19] on the basis of the hypersonic-small-disturbance theory[16] shows that there is a distinctly identifiable region next to the surface, where the pressure gradient normal to the surface almost vanishes. The fluid particles within such a region must have come through a strong portion of the shock wave near the nose, so long as the far downstream of the nose is excluded from our considerations. We thus regard such a region as the entropy layer. When the viscosity effect is introduced, the boundary layer grows along the surface. If the boundary layer is confined within the entropy layer where the normal pressure gradient almost vanishes, the inviscid entropy layer is not identifiable from the boundary layer. For such a case we assume the flow model that the flow field behind the shock wave is made up of two regions: the inviscid hypersonic flow region and the entropy layer accompanying the boundary layer. Apparently the region of validity of such a flow model depends on the Reynolds number, the freestream Mach number, and the wall condition.

Consistently with the pressure behavior near the surface from the inviscid hypersonic solution, we may assume throughout the entropy layer

$$\partial p/\partial y = 0 \tag{2.1}$$

The remaining basic equations are written within the thin-shock-layer approximation[7]—viz.,

$$\begin{gathered}\frac{\partial \rho u}{\partial x} + \frac{\partial \rho v}{\partial y} = 0 \\ \rho u \frac{\partial u}{\partial x} + \rho v \frac{\partial u}{\partial y} = -\frac{\partial p}{\partial x} + \frac{\partial}{\partial y}\left[\mu \frac{\partial u}{\partial y}\right] \\ \rho u \frac{\partial H}{\partial x} + \rho v \frac{\partial H}{\partial y} = \frac{\partial}{\partial y}\left[\frac{\mu}{Pr}\frac{\partial H}{\partial y} + \mu\left(1 - \frac{1}{Pr}\right) u \frac{\partial u}{\partial y}\right]\end{gathered} \tag{2.2}$$

Here the plate surface is the reference surface and coordinates x, y are taken with x measured from the leading edge along the plate and with y normal to it. The velocity components, density, pressure, total enthalpy, and viscosity coefficient are denoted respectively by u, v, ρ, p, H, and μ.

If the outer edge of entropy layer is given by

$$y = y_E$$

we have, from the continuity relation (Fig. 1),

$$\int_0^{y_E} \rho u dy = \rho_\infty u_\infty t + \Psi_E \tag{2.3}$$

where Ψ_E denotes the mass flow which enters the entropy layer across the edge upstream from the point under consideration. The left-hand side is the total mass flow across the entropy layer. Throughout the present paper the subscripts ∞ and E stand for the quantities at the freestream and entropy-layer edge, respectively.

At the wall the usual no-slip condition and constant-temperature condition are applied, that is,

$$u = v = 0, \quad H = H_w \qquad \text{at } y = 0 \tag{2.4}$$

where the subscript w refers to the wall condition. On the other hand, at the edge of entropy layer we require

$$u = u_E, \quad H = H_E \qquad \text{at } y = y_E \tag{2.5}$$

Keeping in mind that the edge of entropy layer is assumed to provide a limit of the validity of hypersonic-small-disturbance theory as one approaches the surface from the inviscid region and that the boundary layer is assumed to be confined within the entropy layer, we have approximately

$$u_E \approx u_\infty, \quad H_E \approx H_\infty \qquad \text{at } y = y_E$$

For convenience, a transformation similar to that in Ref. 13 is introduced, that is,

$$\xi = \int_0^x C \frac{p}{p_\infty}\frac{dx}{t} \tag{2.6a}$$

$$\eta = \sqrt{\frac{Re_t}{\xi}} \int_0^y \frac{\rho}{\rho_\infty} \frac{dy}{t} \tag{2.6b}$$

$$\partial f/\partial \eta = u/u_E \approx u/u_\infty \tag{2.6c}$$

$$\Theta = (H - H_w)/(H_E - H_w) \approx (H - H_w)/(H_\infty - H_w) \tag{2.6d}$$

where

$$Re_t = \rho_\infty u_\infty t/\mu_\infty$$

To simplify the calculation without loss of any essential features, we assume a linear viscosity-temperature relation

$$\mu/\mu_\infty = C(T/T_\infty)$$

and a unit Prandtl number. Then the set of Eqs. (2.2) becomes

$$2f_{\eta\eta\eta} + ff_{\eta\eta} - 2\xi[f_\eta f_{\xi\eta} - f_\xi f_{\eta\eta}] = \epsilon\left[\left(2\frac{dp}{dx}\int_0^x p\,dx\right)/p^2\right]\left[\frac{T_w}{T_0} + \left(1 - \frac{T_w}{T_0}\right)\Theta - f_\eta^2\right] \tag{2.7a}$$

$$2\Theta_{\eta\eta} + f\Theta_\eta - 2\xi[f_\eta\Theta_\xi - f_\xi\Theta_\eta] = 0 \tag{2.7b}$$

where ϵ is the ratio of the freestream density to that across the normal shock wave, that is

$$\epsilon = (\gamma - 1)/(\gamma + 1)$$

With the strong-shock approximation, in the present paper the magnitude of ϵ is assumed small. The conditions, Eqs. (2.3), (2.4), and (2.5), are then transformed respectively into

$$f(\eta_E) = \sqrt{Re_t/\xi}\,(1 + \Psi_E/\rho_\infty u_\infty t) \tag{2.8a}$$

$$f = \partial f/\partial\eta = 0, \quad \Theta = 0 \qquad \text{at } \eta = 0 \tag{2.8b}$$

$$\partial f/\partial\eta = 1, \quad \Theta = 1 \qquad \text{at } \eta = \eta_E \tag{2.8c}$$

where η_E denotes the η coordinate of the outer edge of the entropy layer.

It was pointed out by Lees[17] that for a hypersonic boundary layer with a highly cooled wall the pressure gradient may be small, on the basis of the fact that the term $[T_w/T_0 + (1 - T_w/T_0)\Theta - f_\eta^2]$ is small throughout the layer. In addition, as pointed out in Ref. 13, the factor is of the order of the density ratio ϵ. Therefore, within the framework of the present analysis, the pressure gradient is unimportant for the case of small ϵ.

As can be seen from Eq. (2.8a), $f(\eta_E)$ or η_E becomes large for large Reynolds number Re_t. If the Reynolds number is sufficiently large, so that η_E is relatively large compared to one, say larger than about 4, we can set $\eta \to \infty$ instead of $\eta = \eta_E$ in the condition Eq. (2.8c); that is,

$$\partial f/\partial\eta = 1, \quad \Theta = 1 \qquad \text{at } \eta \to \infty \tag{2.9}$$

For such cases the solution for the entropy layer becomes approximately the same as that of the usual boundary layer. The only difference from the usual boundary-layer problem is in that the mass-flow condition, Eqs. (2.3) or (2.8a), is imposed on the unknown location of the outer edge.†

The outer edge of the entropy layer as well as the surface pressure distribution remain still unknown. By the use of Eq. (2.6b) we have

$$y_E = \sqrt{\frac{\xi}{Re_t}}\,\epsilon t \int_0^{\eta_E} \frac{\rho_0}{\rho}\,d\eta \tag{2.10}$$

where the subscript 0 denotes stagnation conditions behind a normal shock wave. With h the specific enthalpy, the definitions of f and Θ lead to

$$\frac{h}{H_0} = \frac{T}{T_0} = \frac{T_w}{T_0} + \left(1 - \frac{T_w}{T_0}\right)\Theta - f_\eta^2 + \frac{T_E}{T_0} f_\eta^2$$

whence

$$\frac{\rho_0}{\rho} = \frac{T}{T_0}\frac{p_0}{p_E} = \frac{p_0}{p_E}\left[\frac{T_w}{T_0} + \left(1 - \frac{T_w}{T_0}\right)\Theta - f_\eta^2 + \frac{T_E}{T_0} f_\eta^2\right] \tag{2.11}$$

Applying the isentropic relation to a streamline penetrating into the entropy layer across the edge, we obtain

$$T_E/T_{0E} = (p_E/p_{0E})^{1-1/\gamma} \tag{2.12}$$

where subscript 0_E denotes the quantities just behind the shock wave where the streamline concerned leaves the shock (see Fig. 1). Since, from the strong-shock approximation,

$$T_{0E}/T_0 \approx p_{0E}/p_0$$

we have, from Eq. (2.12)

$$\frac{T_E}{T_0} \approx \frac{p_{0E}}{p_0}\left(\frac{p_E}{p_{0E}}\right)^{1-1/\gamma} \tag{2.13}$$

With Eqs. (2.11) and (2.13), Eq. (2.10) is rewritten as

$$y_E = \sqrt{\frac{\xi}{Re_t}}\,\epsilon t \frac{p_0}{p_E}\int_0^{\eta_E}\left[\frac{T_w}{T_0} + \left(1 - \frac{T_w}{T_0}\right)\Theta - f_\eta^2 + \frac{p_{0E}}{p_0}\left(\frac{p_E}{p_{0E}}\right)^{1-1/\gamma} f_\eta^2\right] d\eta \tag{2.14}$$

As was shown before, with the neglect of the pressure term the solution for the entropy layer reduces to the Blasius-type solution, so long as the Reynolds number is sufficiently large so that η_E may be relatively large compared to one. We then have

$$\begin{aligned} &\int_0^{\eta_E} f_\eta^2\,d\eta \approx f(\eta_E) - 2f_{\eta\eta}(0) \\ &I \equiv \int_0^{\eta_E}\left[\frac{T_w}{T_0} + \left(1 - \frac{T_w}{T_0}\right)\Theta - f_\eta^2\right] d\eta \approx \\ &\int_0^{\infty}\left[\frac{T_w}{T_0} + \left(1 - \frac{T_w}{T_0}\right)\Theta - f_\eta^2\right] d\eta \approx \\ &2f_{\eta\eta}(0) + 1.73\,\frac{T_w}{T_0} \quad (\text{for } Pr = 1) \end{aligned} \tag{2.15}$$

Eq. (2.14) therefore becomes

$$y_E = \sqrt{\frac{\xi}{Re_t}}\,\epsilon t \left(\frac{p_{0E}}{p_E}\right)^{1/\gamma} f(\eta_E) + \sqrt{\frac{\xi}{Re_t}}\,\epsilon t \frac{p_0}{p_E} \times \left[I - 2f_{\eta\eta}(0)\frac{p_{0E}}{p_0}\left(\frac{p_E}{p_{0E}}\right)^{1-1/\gamma}\right]$$

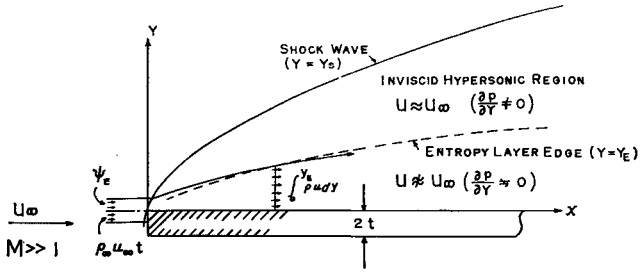

Fig. 1 Illustrative sketch of hypersonic flow over a blunt flat plate

† A similar approach was applied in Ref. 18 to the hypersonic viscous-layer problem of a sharp-leading-edge flat plate.

By the use of the condition, Eq. (2.8a), we obtain from the above equation

$$y_E = \left(\frac{p_{0_E}}{p_E}\right)^{1/\gamma} \epsilon t\,(1 + \Psi_E/\rho_\infty u_\infty t) + \sqrt{\frac{\xi}{Re_t}}\,\epsilon t \times \frac{p_0}{p_E}\left[I - 2f_{\eta\eta}(0)\,\frac{p_{0_E}}{p_0}\left(\frac{p_E}{p_{0_E}}\right)^{1-1/\gamma}\right] \quad (2.16)$$

Evidently p_{0_E} is a function of the stream function $\Psi_E(=\rho_\infty u_\infty y_{S_E}$ where y_{S_E} is the y-coordinate of the point where the concerning streamline leaves the shock wave). The strong-shock-wave approximation gives

$$\frac{p_{0_E}}{p_0} \approx \frac{{y_{S_E}}'^2}{1 + {y_{S_E}}'^2}$$

For the shock wave represented in the form

$$y_S/2t = a(x/2t)^{2/3} \quad (2.17)$$

the ratio of p_{0_E} to the stagnation pressure p_0 can be obtained in terms of Ψ_E as follows:

$$\frac{p_{0_E}}{p_0} \approx \frac{1}{1 + \frac{9}{4a^3}\frac{y_S}{2t}} \approx \frac{1}{1 + \frac{9}{8a^3}\frac{\Psi_E}{\rho_\infty u_\infty t}}$$

The streamlines which reach the entropy-layer edge may reasonably be considered to have initially passed through the strong portion of the shock wave such that ${y_{S_E}}'^2 \gtrsim 1$. Therefore $\Psi_E/\rho_\infty u_\infty t$ is at most of the order of one so that the first term of Eq. (2.16) can be rewritten

$$\left(\frac{p_0}{p_E}\right)^{1/\gamma} \epsilon t \frac{1 + \Psi_E/\rho_\infty u_\infty t}{1 + \frac{9}{8\gamma a^3}\frac{\Psi_E}{\rho_\infty u_\infty t} + 0(\epsilon)} \approx \left(\frac{p_0}{p_E}\right)^{1/\gamma} \epsilon t\left[1 + \left(1 - \frac{9}{8\gamma a^3}\right)\frac{\Psi_E/\rho_\infty u_\infty t}{1 + \Psi_E/\rho_\infty u_\infty t} + 0(\epsilon)\right]$$

because, as will be shown later from the results, $9/8\gamma a^3$ is close to one. For simplicity we shall focus our attention to only the region where

$$1 \gg \left(1 - \frac{9}{8\gamma a^3}\right)\frac{\Psi_E/\rho_\infty u_\infty t}{1 + \Psi_E/\rho_\infty u_\infty t} \quad (2.18)$$

Though this relation may be expected to be valid for ${y_S}'^2 \gtrsim 1$ or $\Psi_E/\rho_\infty u_\infty t \lesssim 1$ so far as the $9/8\gamma a^3$ is very close to one, a more detailed examination on the validity will be given in the succeeding sections. Furthermore the second term in the second square bracket of Eq. (2.16) is assumed negligibly small compared to the first term because, as was mentioned before, the present analysis is based on the assumption that

$$u_E \approx u_\infty \text{ or } (p_E/p_{0_E})^{1-1/\gamma} \ll 1 \quad (2.19)$$

With the foregoing approximations, Eqs. (2.18) and (2.19), Eq. (2.16) becomes

$$y_E \approx \left(\frac{p_0}{p_E}\right)^{1/\gamma} \epsilon t + \frac{p_0}{p_E}\sqrt{\frac{\xi}{Re_t}}\,\epsilon t\, I$$

or with ξ of Eq. (2.6a)

$$\frac{y_E}{2t} \approx \left(\frac{p_0}{p_E}\right)^{1/\gamma} \epsilon t\left[1 + \sqrt{\frac{4\gamma}{\gamma+1}}\left(\frac{p_0}{p_E}\right)^{1-1/\gamma} \times \left(\int_0^x \frac{p_0}{p_E}\frac{dx}{2t}\right)^{1/2}\frac{M\sqrt{C}}{\sqrt{Re_t}}\,I\right] \quad (2.20)$$

The location of the entropy-layer edge can be determined by the above relation independently of Ψ_E from the surface-pressure distribution when the parameters involved are given. As is easily shown, the second term on the right-hand side is identical with the displacement thickness of the boundary layer which grows within the first term and is associated with the displacement effect due to the nose bluntness. In the present paper the entropy layer has been dealt with without separating the inviscid region and the boundary layer. Nevertheless the entropy-layer edge has been found to be a linear combination of both displacement effects due to the inviscid entropy layer and boundary layer, so far as the underlying assumptions are valid.

III. The Matching Procedure of the Entropy-Layer Solution with the Inviscid Hypersonic Solution

We shall now examine the solution for the hypersonic flow ambient to the entropy layer. We tentatively assume the shock-wave shape which is given by $y_S \sim x^{2/3}$. For such a shock wave the hypersonic-small-disturbance theory provides the solution in terms of the similarity variable θ; that is

$$\theta = y/y_S$$

The stream function Ψ defined by

$$\Psi_y = \rho u \approx \rho u_\infty,\ \Psi_x = -\rho v$$

can be obtained in the form

$$\Psi = y_S F(\theta) \quad (3.1)$$

and then the pressure is given (for example, see Refs. 2, 15, and 24) by

$$\frac{p}{p_S} = \left(\frac{\gamma-1}{\gamma+1}\right)^\gamma F'^\gamma/F$$

According to the results, we have for small θ or for the vicinity of the surface

$$F(\theta) = A\theta^{\gamma/(\gamma-1)}[1 + 0(\theta^{(2\gamma-1)/(\gamma-1)})] \quad (3.2a)$$

$$\frac{p}{p_S} = K[1 + 0(\theta^{(2\gamma-1)/(\gamma-1)})] \quad (3.2b)$$

where

$$K = \left(\frac{\gamma}{\gamma+1}\right)^\gamma A^{\gamma-1} \quad (3.2c)$$

The difference of p/p_S from the constant value K is very small over a region next to the surface, because it is of the order of $\theta^{1/\epsilon}$. Indeed the numerical results show that the pressure ratio p/p_S is nearly constant over a distinctly identifiable region next to the surface. We can therefore identify this asymptotic value of the pressure with the pressure p_E across the entropy layer. With the strong-shock approximation, therefore, the pressure p_E is given by

$$\frac{p_E}{p_0} = K\frac{p_S}{p_0} = K\left(\frac{dy_S}{dx}\right)^2 \quad (3.3)$$

We shall first examine the limiting case when Re_t is sufficiently large so that the boundary layer is negligibly thin. The condition, Eq. (2.20), then reduces to

$$y_E \approx (p_0/p_E)^{1/\gamma}\,\epsilon t \quad (3.4)$$

We note that a similar relation between y_E and $(p_0/p_E)^{1/\gamma}$ has been found in Refs. 6 and 13, but with undetermined multiplicative factor. The shock wave has been initially assumed to be of the form

$$y_S/2t = a(x/2t)^{2/3}$$

with a constant a. As will be seen below, in fact the shock wave is obtained in the form

$$y_S/2t = a(x)(x/2t)^{2/3}$$

That is, from Eq. (3.4) with $da(x)/dx \ll 1$

$$a(x) = \left(\frac{3}{2\sqrt{K}}\right)^{2/(2+\gamma)} \left(\frac{\epsilon}{2}\frac{y_S}{y_E}\right)^{2/(2+\gamma)} \left(\frac{x}{2t}\right)^{2(1-\gamma)/3(2+\gamma)} \tag{3.5}$$

Based upon the local similarity concept, however we may expect that the inviscid solution for the case of shock-wave shape with a constant a can also be applied to the present case so long as a is a very slowly varying function of $x/2t$. Indeed $a(x)$ above obtained indicates no appreciable change over a large extent so long as the specific-heat ratio is close to one. Moreover, $a(x)$ is approximately given by

$$a \approx a^* = \left(\frac{3}{2\sqrt{K}}\right)^{2/(2+\gamma)} \left(\frac{\epsilon}{2}\frac{y_S}{y_E}\right)^{2/(2+\gamma)}$$

over a range where

$$\frac{2(1-\gamma)}{3(2+\gamma)} \log\left|\frac{x}{2t}\right| \ll 1$$

According to the results of the hypersonic small-disturbance theory, as was mentioned before, there exists a distinctly identifiable region next to the surface, where the pressure is nearly constant across the layer. Since in the present paper such a region is regarded as the entropy layer, the values of y_E/y_S as well as K can be determined from the result of the hypersonic-small-disturbance theory. With these constants, we obtain the unknown shock-layer-thickness parameter a by the use of Eq. (3.5). Once the shock-wave shape is determined, the pressure p_E and the entropy-layer edge y_E can easily be determined. For example the pressure is

$$\frac{p_E}{p_\infty} = \frac{8\gamma}{9(\gamma+1)} Ka^2M^2\left(\frac{x}{2t}\right)^{-2/3} \tag{3.6}$$

We shall next proceed to examine cases when the boundary-layer-displacement effect is not negligibly small. For these cases the second term in the square bracket of Eq. (2.20) becomes, with p_E from Eq. (3.3)

$$\delta a^{(1-\gamma)/\gamma} \frac{M\sqrt{C}}{\sqrt{Re_t}} I \left(\frac{x}{2t}\right)^{1/6+2(\gamma-1)/3\gamma}$$

where

$$\delta = \left(\frac{4}{9}\right)^{1/\gamma} \sqrt{\frac{\gamma}{\gamma+1}} K^{\frac{2-\gamma}{2\gamma}}$$

Therefore, combining Eq. (2.18) with p_E/p_0 from Eq. (3.3) we obtain the relation similar to Eq. (3.5) as follows:

$$a = \left(\frac{3}{2\sqrt{K}}\right)^{2/(2+\gamma)} \left(\frac{\epsilon}{2}\frac{y_S}{y_E}\right)^{2/(2+\gamma)} \left[1 + \delta a^{(1-\gamma)/\gamma} \frac{M\sqrt{C}}{\sqrt{Re_t}} I \left(\frac{x}{2t}\right)^{1/6+2(\gamma-1)/3\gamma}\right]\left(\frac{x}{2t}\right)^{2(1-\gamma)/3(2+\gamma)} \tag{3.7}$$

As in the previous case, a is not strongly dependent on $x/2t$, so far as the boundary layer is still thin in comparison with the entropy-layer thickness. Indeed the numerical results for the case of $\gamma = 1.4$ show that a of Eq. (3.7) indicates no appreciable dependence on $x/2t$ over a certain extent which depends on the values of $M\sqrt{C}/\sqrt{Re_t}$ and I or T_w/T_0.

We must here discuss the validity of the condition Eq. (2.18) which was assumed in the derivation of Eq. (2.20) or (3.7). The stream function is given from the definition

$$\Psi_E = \int_0^{y_E} \rho_{inv.}\, u_{inv.}\, dy$$

where the subscripts *inv.* stand for quantities given by the inviscid solution. By the use of Eqs. (3.1) and (3.2a),

$$\Psi_E = y_S\rho_\infty u_\infty \int_0^{\theta_E} F'(\theta)d\theta = u_\infty\rho_\infty y_S F(\theta_E) \approx Au_\infty\rho_\infty y_S\theta_E^{\gamma/(\gamma-1)} \tag{3.8}$$

where

$$\theta_E = y_E/y_S$$

Therefore the condition Eq. (2.18) becomes

$$1 \gg \frac{2\left(1 - \frac{9}{8\gamma a^3}\right) Aa\left(\frac{x}{2t}\right)^{2/3}\left(\frac{y_E}{y_S}\right)^{\gamma/(\gamma-1)}}{1 + 2Aa\left(\frac{x}{2t}\right)^{2/3}\left(\frac{y_E}{y_S}\right)^{\gamma/(\gamma-1)}} \tag{3.9}$$

For the case of γ close to one, $(y_E/y_S)^{\gamma/(\gamma-1)}$ is very small in comparison with one because y_E/y_S is smaller than one. Moreover, as will be shown later, the remaining constant factor $\{1 - [9/(8\gamma a^3)]\}$ is found to be smaller than one. Therefore the above condition may be expected to be sufficiently valid over a certain large extent in terms of $x/2t$. This will be checked by means of our numerical results.

IV. Surface Pressure and Surface Heat-Transfer Rate

In the present analysis the pressure is assumed constant across the entropy layer, so that the pressure p_E at the outer edge of the entropy layer is taken equal to the surface pressure p_w. From Eq. (3.6) we have

$$\frac{p_w}{p_\infty} \approx \frac{p_E}{p_\infty} = \frac{8\gamma}{9(\gamma+1)} Ka^2M^2\left(\frac{x}{2t}\right)^{-2/3} \tag{4.1}$$

In Section II we saw that the solution for the entropy layer can be reduced to that of the usual boundary-layer-type problem when the η_E is relatively large in comparison with one, say larger than about 4. We then have

$$f(\eta_E) \approx \eta_E - \beta$$

where $\beta = 1.7$ for the Blasius-type solution. With this relation Eq. (2.8a) gives

$$\eta_E \approx \sqrt{Re_t/\xi}\,(1 + \Psi_E/\rho_\infty u_\infty t) + \beta$$

Since ξ and $\Psi_E/\rho_\infty u_\infty t$ are given by Eqs. (2.6a) and (3.8), respectively, the above relation becomes

$$\eta_E \approx \frac{1}{4a}\sqrt{\frac{3(\gamma+1)}{\gamma K}} \frac{\sqrt{Re_t}}{M\sqrt{C}} \left(\frac{x}{2t}\right)^{-1/6} \times \left[1 + 2Aa\left(\frac{x}{2t}\right)^{2/3}\left(\frac{y_E}{y_S}\right)^{\gamma/(\gamma-1)}\right] + \beta \tag{4.2}$$

In order that the entropy-layer solution be reduced to that for the usual boundary-layer problem, $\sqrt{Re_t}/M\sqrt{C}$ must be sufficiently large so that the η_E is relatively large in comparison with one over a large extent in terms of $x/2t$. For such cases the surface heat-transfer coefficient defined by

$$C_H = (\lambda\partial T/\partial y)_w/\rho_\infty u_\infty(H_\infty - H_w)$$

is given in quite the same way as in the usual boundary-layer problem. That is, for the unit Prandtl number[13]

$$M^3C_H \approx f_{\eta\eta}(0)M^3\sqrt{C}/\sqrt{Re_t}(p_E/p_\infty)\left(\int_0^x p_E\,dx/p_\infty t\right)^{-1/2}$$

With p_w/p_∞ of Eq. (4.1) we have

$$M^3C_H \approx \frac{f_{\eta\eta}(0)}{\sqrt{3}}\sqrt{\frac{8\gamma K}{9(\gamma+1)}}\, a\bar{\chi}M\left(\frac{2t}{x}\right)^{1/3} \tag{4.3}$$

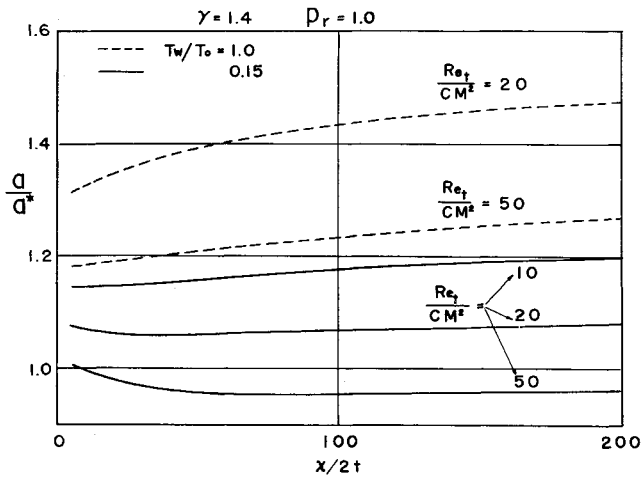

Fig. 2 The ratio of the shock-layer-thickness parameter a to the reference value a^* when the Reynolds number is very large

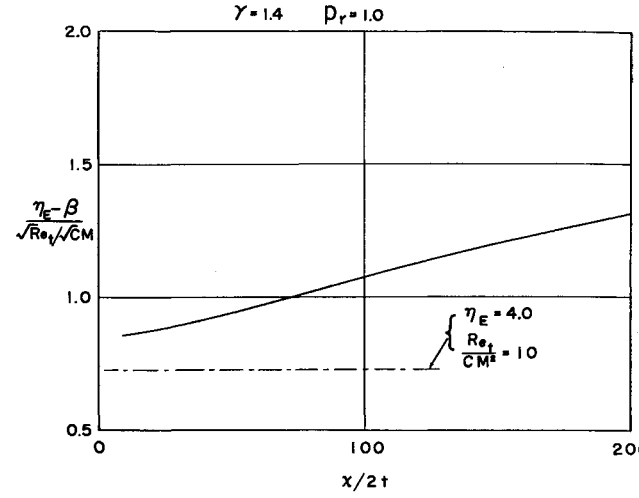

Fig. 3 The value of η_E, the η-coordinate of the entropy layer edge

where $\bar{\chi}$ is the hypersonic interaction parameter[8]

$$\bar{\chi} = \frac{M^3\sqrt{\bar{C}}}{\sqrt{Re_x}}$$

V. Numerical Results and Examination of the Validity of the Analysis

The calculation has been carried out for the case of $\gamma = 1.4$. The solution for the inviscid hypersonic flow behind the power-law shock wave which is given by $y_S \sim x^{2/3}$ has been obtained by Kubota.[19] In applying the hypersonic equivalence principle, the numerical result of this solution for a steady hypersonic flow reduces to quite the same as that for the constant-energy blast wave, which was investigated by Sedov,[20] Sakurai,[21] and Lin.[22] The results for the case $\gamma = 1.4$ give

$$(p/p_S)_{y/y_S \to 0} = 0.390$$

Since the pressure should tend to the surface value $p_w (\approx p_E)$ as $y/y_S \to 0$, we obtain the constant K and A from Eqs. (3.2b) and (3.2c). From the numerical result shown in Ref. 2, there certainly exists an identifiable region next to the surface, where p/p_S indicates no appreciable change. Actually y_E/y_S has been chosen as the point where the fractional deviation of the pressure from the surface value is one percent. We thus obtain

$$y_E/y_S \approx 0.40$$

With these values of K and y_E/y_S above obtained, the shock-layer-thickness parameter a^* has been evaluated by the use of Eq. (3.5) for the limiting case when Re_t is extremely large so that the boundary-layer displacement effect may be neglected. That is,

$$a^* = 0.878$$

and then the surface pressure p_w is given, from Eq. (4.1), by

$$\frac{p_w}{p_\infty} = 0.156M^2\left(\frac{2t}{x}\right)^{2/3}$$

For the case when the boundary-layer displacement effect is not negligibly small, the shock-layer-thickness parameter a can be determined from Eq. (3.7). The factor $a^{(1-\gamma)/\gamma}$ appearing in Eq. (3.7) can be replaced by $a^{*(1-\gamma)/\gamma}$ without any significant error because the exponent is very small in the order of ϵ. As can be seen from Eq. (2.15), the factor I appearing in Eq. (3.7) depends on the wall-to-stagnation temperature ratio. For the Blasius-type solution we have

$$I = 0.664 + 1.73\, T_w/T_0$$

The ratios of a to a^* have been calculated for typical values of $M\sqrt{C}/\sqrt{Re_t}$ and T_w/T_0. In Fig. 2 is plotted the ratio of a to a^* against $x/2t$.

We must recall that Eq. (3.7) has been derived on the assumption that a is a very slowly function of $x/2t$. We can see from Fig. 2 that this assumption is approximately assured over a range depending on the values of both the parameters Re_t/M^2C and T_w/T_0. Indeed the a's indicate no appreciable change over quite a large range in terms of $x/2t$, for $Re_t/M^2C \gtrsim 10$ when $T_w/T_0 = 0.15$ and for $Re_t/M^2C \gtrsim 50$ when $T_w/T_0 = 1.0$. As is also seen from Fig. 2, the shock-wave shape is relatively insensitive to the variation of Re_t/M^2C for a fixed T_w/T_0. In other words the inviscid region seems to be not strongly affected due to the boundary-layer growth within the entropy layer.

We should also recall the assumption that η_E is relatively large in comparison with one. In order to estimate the magnitude of η_E, Eq. (4.2) can be applied. We then set a on the right-hand side to one. The values of $(\eta_E - \beta)/(\sqrt{Re_t}/M\sqrt{C})$ thus obtained are plotted against $x/2t$ in Fig. 3. We can see from the result shown in this figure that when Re_t/M^2C for any wall-to-stagnation temperature ratio, η_E is so large that the boundary layer may be imbedded within the entropy layer. The remaining main assumption is the validity of the condition, Eqs. (2.18) or (3.9), in which case Eq. (2.16) may be approximated by Eq. (2.20). This can be checked by the use of Eq. (3.9). Indeed the neglect of this factor lead to only a small error, less than a few percent in the value of a, over the range under consideration.

In Refs. 13 and 14 Cheng et al. presented, based on the blast-wave analogy, an analysis on the effects of both bluntness and viscosity in a hypersonic flow over blunt-nosed bodies, and, moreover, compared with the data on surface heat-transfer rate which were obtained by their Shock-tunnel experiment. Their theoretical results were also compared with the data on surface pressure obtained at the same laboratory.[23] We shall compare our results with both the theoretical and experimental results worked out by the group of Cornell Aeronautical Lab.

The surface pressure and heat-transfer rate were calculated by the use of Eqs. (4.1) and (4.3), respectively, with values of the shock-layer-thickness parameter a associated closely with the experimental conditions. In Ref. 23 the surface pressure was measured over a range where $1 \lesssim x/2t \lesssim 20$, for the case of $\gamma = 1.4$, $Re_t/M^2C \approx 50$, and $T_w/T_0 \approx 0.15$. For this condition the shock-layer-thickness parameter has been chosen from the results shown in Fig. 2—viz.,

$$a/a^* \approx 1.0 \quad \text{or} \quad a \approx 0.878$$

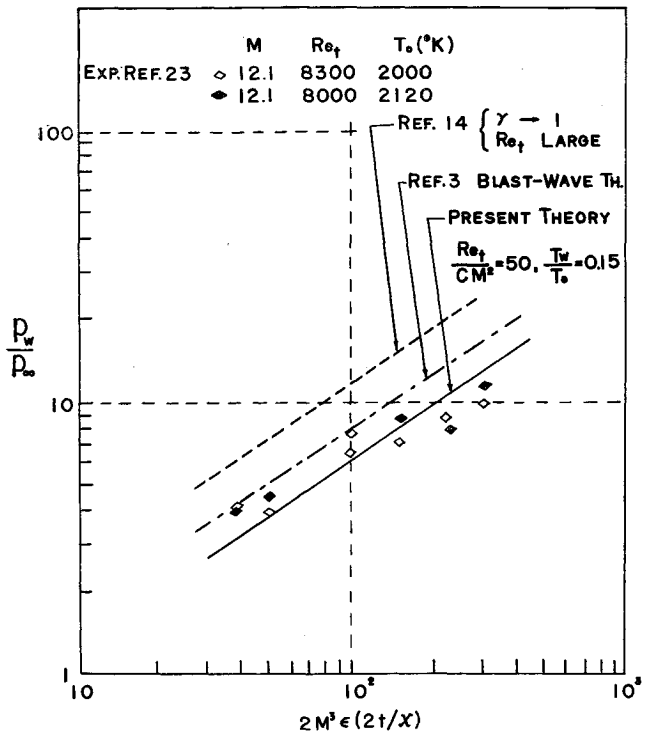

Fig. 4 The pressure distribution along the plate surface

By the use of this value of a the surface pressure has been evaluated from Eq. (4.1) as

$$\frac{p_w}{p_\infty} \approx 0.156M^2\left(\frac{x}{2t}\right)^{-2/3}$$

This is plotted in Fig. 4‡ with the results in Refs. 14 and 23. The corresponding heat-transfer coefficient is thus given from Eq. (4.3); viz.,

$$M^3C_H \approx 0.076\frac{M^3\sqrt{C}}{\sqrt{Re_x}}\left(\frac{M^32t}{x}\right)^{1/3}$$

In quite a similar way the heat-transfer coefficient of Eq. (4.3) is determined for two other cases of $Re_t/M^2C \approx 10$ and $20(\gamma = 1.4,\ T_w/T_0 \approx 0.15,\ 5 \lesssim x/2t \lesssim 100)$—viz., for $Re_t/M^2C \approx 10$

$$a/a^* \approx 1.17 \quad M^3C_H \approx 0.089\frac{M^3\sqrt{C}}{\sqrt{Re_x}}\left(\frac{M^32t}{x}\right)^{1/3}$$

for $Re_t/M^2C \approx 20$

$$a/a^* \approx 1.07 \quad M^3C_H \approx 0.081\frac{M^3\sqrt{C}}{\sqrt{Re_x}}\left(\frac{M^32t}{x}\right)^{1/3}$$

These calculated values of the heat-transfer coefficient are plotted in Fig. 5.

For comparison the theoretical results of Ref. 14 are also plotted in Figs. 4 and 5. The present results for the heat-transfer coefficient show relatively lower values than either the experimental data or the results of Ref. 14. As regards the surface pressure the results of the present analysis agree satisfactorily with the experimental data (see Fig. 4). As was mentioned before, some uncertainty in the determination of the nose-drag coefficient k is inevitably involved in any analysis incorporating the blast-wave analogy. As can be

‡ In Refs. 14 and 23 the experimental data on the surface pressure and heat-transfer rate were plotted against $M^3\epsilon k2t/x$ and $(M^3\epsilon k2t/x)^{1/3}\bar{\chi}$ with $k = 2$, respectively, where k is the nose-drag coefficient. For convenience the same plots are used in Figs. 4 and 5.

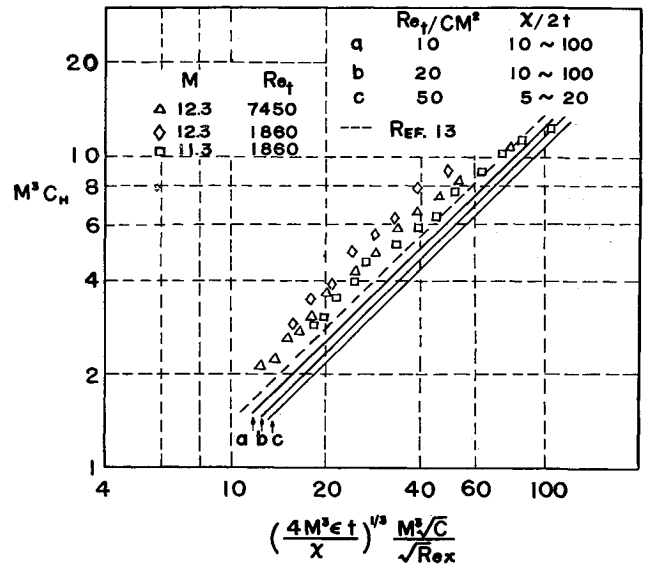

Fig. 5 The surface heat-transfer coefficient

seen from Figs. 4 and 5, the theoretical result of Ref. 14 for $k = 2$ gives a higher estimate of the surface pressure, while it gives a lower estimate of the surface heat-transfer coefficient in comparison with the experimental data. However, for any choice of the value of k the results could not be made to fit the experimental data regarding both the surface pressure and the heat-transfer rate. It is worthwhile noting that the results of the present analysis, which is not based on the blast-wave analogy, involve no semi-empirical factor such as k.

In summarizing, the present analysis was based on the following flow model: the fluid particles that passed through a strong portion of the shock wave above the nose shoulder constitute the entropy-layer edge which divides the flow field behind the shock wave into the inviscid hypersonic flow region and entropy layer, and the boundary layer is so thin that it is confined within the entropy layer. If such a flow model is assumed, the shock wave is found to be of the form

$$y_S/2t = a(x/2t)^{2/3}$$

in which a is very slowly varying with $x/2t$ so that may be regarded as a constant over a certain region. Then the inviscid hypersonic solution has been shown to be approximately matched with the entropy-layer solution. The existence of such a flow model has been justified in a certain region of $x/2t$ whose extent can be determined from the imposed conditions on the validity of the present model when γ, T_w/T_0 and Re_t/M^2C are given. In conclusion it is hoped that a simplifying analysis presented here will provide a clue to make clearer some of the essential features of the hypersonic flow over a blunt-nosed flat plate.

References

[1] Lees, L., "Inviscid hypersonic flow over blunt-nosed slender bodies," GALCIT Memo. 31 (Feb. 1956).

[2] Lees, L. and Kubota, T., "Inviscid hypersonic flow over blunt-nosed slender bodies," J. Aeron. Sci. **24**, 195 (March 1957).

[3] Cheng, H. K. and Pallone, A. J., "Inviscid leading-edge effect in hypersonic flow," J. Aeron. Sci. **23**, 700 (July 1956).

[4] Chernyi, G. G., "Hypersonic flow past an airfoil with a slightly blunted leading edge," Dokl. Akad. Nauk USSR **114**, 721 (1957).

[5] Lunev, V. V., "Motion of a slender blunted body in the atmosphere with high supersonic speed," Izv. Akad. Nauk USSR, Otd. Tekhn. Nauk, Mekhan. i Mashinostr. 131 (1959); ARS J. **30**, 414 (April 1960).

[6] Sychev, V. V., "On the theory of hypersonic gas flow with a

power-law shock wave," Prikl. Math. i Mekhan. **24**, 518 (1960); J. Appl. Math. and Mech. **24**, 756 (1960); see also Probstein, R. F., "Recent Soviet advances in inviscid hypersonic aerodynamics," Aerospace Eng. **20**, 10 (July 1961).

[7] Hayes, W. D., "On hypersonic similitude," Quart. Appl. Math. **5**, 105 (1947).

[8] Hayes, W. D. and Probstein, R. F., *Hypersonic Flow Theory* (Academic Press, New York, 1959).

[9] Bertram, M. H., "Viscous and leading-edge thickness effects on the pressure on the surface of a flat plate in hypersonic flow," J. Aeron. Sci. **21**, 430 (June 1954).

[10] Hammitt, A. G., Vas, I. E., and Bogdonoff, S. M., "Leading-edge effects on the flow over a flat plate at hypersonic speeds," Princeton Aeron. Eng. Rept. 326 (1955).

[11] Hammitt, A. G. and Bogdonoff, S. M., "Leading-edge effect on the flow over a flat plate," Jet Propulsion **26**, 241 (May 1956).

[12] Creager, M. O., "Effects of leading-edge blunting on the local heat transfer and pressure distribution over flat plates in supersonic flow," NACA TN4142 (Dec. 1957).

[13] Cheng, H. K., "Hypersonic flow with leading-edge bluntness and boundary layer displacement effects," ONR-Sponsored Cornell Aeron. Lab. Rept. AF 1285-A-4 (Aug. 1960).

[14] Cheng, H. K., Hall, J. G., Golian, T. C., and Herzberg, A., "Boundary-layer displacement and leading-edge bluntness effects in high-temperature hypersonic flow," J. Aerospace Sci. **28**, 353 (May 1961).

[15] Mirels, H. and Thornton, P. R., "Effects of body perturbations on hypersonic flow over slender, power-law bodies," NASA TR R-45 (May 1959).

[16] Van Dyke, M. D., "Application of hypersonic small-disturbance theory," J. Aeron. Sci. **21**, 179 (March 1954); also NACA TR 1194 and NACA TN 3173.

[17] Lees, L., "Laminar heat transfer over blunt-nosed bodies at hypersonic flight speeds," Jet Propulsion **26**, 259 (April 1956).

[18] Oguchi, H., "The sharp leading edge problem in hypersonic flow," *Rarefied Gas Dynamics*, edited by L. Talbot (Academic Press, New York, 1961); see also Brown University Rept., ARL TN 60-133 (Aug. 1960).

[19] Kubota, T., "Investigation of flow around simple bodies in hypersonic flow," GALCIT Memo. 40 (June 1957).

[20] Sedov, L. I., *Similarity and Dimensional Methods in Mechanics* (Gostekhizdat, Moscow, 1957), 4th ed.; transl. edited by M. Holt (Academic Press, New York, 1959).

[21] Sakurai, A., "On the propagation and structure of the blast wave—part I," J. Phys. Soc. (Japan) **9**, 256 (March-April 1954).

[22] Lin, S. C., "Cylindrical shock wave produced by instantaneous energy release," J. Appl. Phys. **25**, 54 (Jan. 1954).

[23] Hall, J. G. and Golian, T. C., "Shock-tunnel studies of hypersonic flat-plate airflows," Cornell Aeron. Lab. Rept., AD-1052-A-10 (Dec. 1960).

[24] Oguchi, H., "First-order approach to a strong interaction problem in hypersonic flow over an insulated flat plate," University of Tokyo, Aeron. Res. Inst. Rept. 330 (June 1958).

FEBRUARY 1963 AIAA JOURNAL VOL. 1, NO. 2

Some Applications of Detailed Wind Profile Data to Launch Vehicle Response Problems

HOMER G. MORGAN* AND DENNIS F. COLLINS JR.*

NASA Langley Research Center, Hampton, Va.

The response of a launch vehicle to a number of detailed wind profiles has been determined. The wind profiles were measured by two techniques that are described briefly. One of these techniques uses an angle-of-attack sensor in conjunction with guidance data to measure the wind profile traversed by some particular launch vehicle. The other wind-measuring technique is a photographic triangulation method, whereby two cameras take simultaneous pictures of a vertical trail of smoke left by a launch vehicle or sounding rocket. The response of a vehicle flying these detailed profiles is compared with the response of the same vehicle flying through balloon-measured profiles. The response to the detailed wind profiles, relative to the balloon-measured profiles, is characterized by the large excitation of the rigid pitch and elastic bending modes. This is found to cause higher loads on the launch vehicle structure. Established design criteria that use balloon-measured wind profiles have accounted for this increased load arbitrarily by adding a load due to some type of discrete gust.

Nomenclature

M = bending moment, lb-in.
M_{detailed} = bending moment induced by a detailed wind profile, lb-in.
M_{limit} = limit bending moment, lb-in.
M_{smoothed} = bending moment induced by a balloon-type wind profile, lb-in.
V_a = relative airstream velocity, fps
V_i = inertial velocity, fps
V_w = wind velocity, fps
y = translation normal to a reference trajectory, in.
α = angle of attack, rad
γ = flight-path angle, rad
θ = attitude angle, rad

Presented at the ARS Launch Vehicles: Structures and Materials Conference, Phoenix, Ariz., April 3–5, 1962; revision received November 1, 1962.

* Aerospace Technologist.

Introduction

THE wind and gust criteria for determining design loads on launch vehicles and the analytical methods by which these criteria are applied reflect the characteristics of available wind and gust data. The wind data have been obtained primarily from balloon soundings that detect only the gross motion of the atmosphere and filter out the small-scale fluctuations as indicated in Fig. 1. Examples of design criteria based on such wind data are the synthetic wind profiles of Refs. 1–4 and the measured profiles in Refs. 3 and 5. Most of the gust data that have been available were for vertical gusts (or turbulence) measured by a horizontally flying airplane,[6–8] also